Two-Dimensional NMR Studies of Staphylococcal Nuclease. 1. Sequence-Specific Assignments of Hydrogen-1 Signals and Solution Structure of the Nuclease H124L–Thymidine 3′,5′-Bisphosphate–Ca^{2+} Ternary Complex†

Jinfeng Wang,‡ David M. LeMaster,§ and John L. Markley*,‡

Department of Biochemistry, College of Agricultural and Life Sciences, University of Wisconsin—Madison, 420 Henry Mall, Madison, Wisconsin 53706, and Department of Biochemistry, Molecular Biology and Cell Biology, Northwestern University, Evanston, Illinois 60208

Received June 12, 1989

ABSTRACT: Staphylococcal nuclease H124L is a recombinant protein produced in *Escherichia coli* whose sequence is identical with that of the nuclease produced by the V8 variant of *Staphylococcus aureus*. The enzyme–metal ion activator–nucleotide inhibitor ternary complex, nuclease H124L–thymidine 3′,5′-bisphosphate–Ca^{2+}, was investigated by two-dimensional (2D) NMR techniques. Efficient overproduction of the enzyme facilitated the production of random fractionally deuterated protein, which proved essential for detailed NMR analysis. ^1H NMR spin systems were analyzed by conventional 2D $^1H\{^1H\}$ methods: COSY, relayed COSY, HOHAHA, and NOESY. Assignments obtained by ^1H NMR experiments were confirmed and extended by ^1H–^{13}C and ^1H–^{15}N heteronuclear NMR experiments [Wang, J., Hinck, A. P., Loh, S. N., & Markley, J. L. (1990) *Biochemistry* (following paper in this issue)]. Spectra of the ternary complexes prepared with protein at natural abundance and at 50% random fractional deuteration provided the information needed for sequence-specific assignments of 121 of the 149 amino acid residues. Short- and intermediate-range NOE connectivities allowed the determination of secondary structural features of the ternary complex: three α-helical domains and three antiparallel β-pleated sheets with several reverse turns. A number of nonsequential long-range H^N–H^N and H^α–H^N connectivities revealed additional information about the spatial arrangement of these secondary structural elements. The solution structure of this ternary complex shows a close correspondence to the crystal structure of the nuclease wt–thymidine 3′,5′-bisphosphate–Ca^{2+} ternary complex [Cotton, F. A., Hazen, E. E., & Legg, M. J. (1979) *Proc. Natl. Acad. Sci. U.S.A. 76*, 2551–2555].

Fundamental questions in protein chemistry concern the relationships linking amino acid sequence, three-dimensional structure, and enzyme function. Since the mid 1960s, staphylococcal nuclease has served as a model system for such investigations (Anfinsen, 1973). It was chosen because it is a relatively small single-chain protein that lacks cysteine and is reversibly denaturable. Jardetzky and co-workers used staphylococcal nuclease for early NMR[1] investigations of protein conformational equilibria (Markley et al., 1970) and protein folding (Jardetzky et al., 1972); the latter studies employed selective deuteration strategies for spectral simplification (Markley et al., 1968). Cotton et al. (1979) determined the X-ray structure of an inhibited form of the enzyme which has served as a valuable framework for enzymological and structural studies of the enzyme in solution.

Interest in staphylococcal nuclease has revived sharply in recent years as the result of cloning and mutagenesis studies initiated by Shortle (Shortle, 1983; Shortle & Lin, 1985) and extended by Gerlt (Takahara et al., 1985), Fox (1986), and others (Uhlmann & Smith, 1987; Alexandrescu et al., 1988). These investigations have focused on protein stability (Claderon et al., 1985; Shortle, 1986; Shortle & Meeker, 1986), protein dynamics (McCain & Markley, 1988), the roles of active-site residues (Serpersu et al., 1987; Grissom & Markley, 1989), and protein conformation (Stanczyk et al., 1988; Wilde et al., 1988). Mutagenesis studies of conformational equilibria linking two native forms of the enzyme (N/N′) and two denatured forms (U/U*) suggest that they differ by a *cis/trans* equilibrium about the Lys^{116}–Pro^{117} peptide bond (Fox et al.,

† Supported by Grants GM35976 and GM38779 from the National Institutes of Health. This study made use of the National Magnetic Resonance Facility at Madison which is supported in part by NIH Grant RR02301 from the Biomedical Research Technology Program, Division of Research Resources. Equipment in the facility was purchased with funds from the University of Wisconsin, the NSF Biological Biomedical Research Technology Program (DMB-8415048), the NIH Biomedical Research Technology Program (RR02301), the NIH Shared Instrumentation Program (RR02781), and the U.S. Department of Agriculture. Preliminary results were presented at the XIIIth International Conference on Magnetic Resonance in Biological Systems, Madison, WI, Aug 14–19, 1988.

‡ University of Wisconsin—Madison.

§ Northwestern University.

[1] Abbreviations: COSY, 2D correlated spectroscopy; 2D, two dimensional; DQF, double quantum filtered; FID, free induction decay; HOHAHA, two-dimensional Hartmann–Hahn magnetization transfer spectroscopy; $^1H\{^{13}C\}$SBC, two-dimensional ^1H-detected ^1H–^{13}C single-bond correlation; $^1H\{^{13}C\}$SBC-NOE, two-dimensional ^1H-detected ^1H–^{13}C single-bond correlation with NOE relay; $^1H\{^{15}N\}$SBC, two-dimensional ^1H-detected ^1H–^{15}N single-bond correlation; $^1H\{^{15}N\}$SBC-NOE, two-dimensional ^1H-detected ^1H–^{15}N single-bond correlation with NOE relay; NMR, nuclear magnetic resonance; NOE, nuclear Overhauser enhancemnt; NOESY, 2D NOE spectroscopy; nuclease H124L, mutant of the nuclease from *Staphylococcus aureus* (Foggi strain) (EC 3.14.7) in which the histidine at residue 124 has been replaced with leucine; H124L-TC, nuclease H124L–pdTp–Ca^{2+} ternary complex; [na]H124L-TC, ternary complex prepared with natural abundance (unlabeled) nuclease H124L; [50% ul ^2H]H124L-TC, ternary complex prepared with 50% random fractionally deuterated nuclease H124L; pdTp, thymidine 3′,5′-bisphosphate; RCT-COSY, relayed coherence transfer spectroscopy; TSP, 3-(trimethylsilyl)propionate-d_4. Cross-peak positions in spectra are given as x,y ppm where x is the horizontal axis and y is the vertical axis.

0006-2960/90/0429-88$02.50/0

1986; Evans et al., 1987, 1989). The positions of these equilibria are affected profoundly by certain single-site mutations located at various distances from the loop containing Pro^{117} (Alexandrescu et al., 1989), and a linkage between the conformational change and the global stability of the enzyme has been established (A. T. Alexandrescu, A. P. Hinck, and J. L. Markley, unpublished results). Additional X-ray studies of the wild-type enzyme (Loll & Lattman, 1989) and its mutants (Loll et al., 1988; Hynes et al., 1989) have been undertaken.

Detailed NMR investigations of different recombinant forms of staphylococcal nuclease as ternary complexes (nuclease–pdTp–Ca^{2+}) are underway in our laboratory and independently in that of Dr. D. A. Torchia (National Institutes of Health). The Torchia laboratory has used the Hibler et al. (1987) construct which produces protein having the sequence of the nuclease from the Foggi strain of *Staphylococcus aureus* (defined here as nuclease wt) but containing an amino-terminal heptapeptide extension.[2] They have used a perdeuteration method along with selective ^{15}N labeling to study the helical regions of the protein (Torchia et al., 1988) and are employing ^{13}C and ^{15}N labeling strategies to obtain further sequence-specific assignments (Torchia et al., 1989).

Our laboratory is using the Shortle (1983) construct which lacks the amino-terminal extension. We have chosen nuclease H124L (the enzyme whose sequence is identical with that of the nuclease isolated from the V8 strain of *S. aureus*) as a starting sequence for structural studies because this protein has a higher thermal stability than nuclease wt (Alexandrescu et al., 1989). We report here the sequence-specific assignment of 121 out of 149 residues and an analysis of the secondary structure and global fold of the protein (as the ternary complex) in solution. We found it extremely difficult to assign the ^1H NMR spectrum by classical two-dimensional NMR methods (Wüthrich, 1986) and found it necessary to take advantage of the spectral simplification afforded by random fractional deuteration (LeMaster & Richards, 1988). The ^1H NMR spin system assignments have been confirmed and extended by a concerted multinuclear 2D NMR spectroscopy approach (Stockman et al., 1989). Sequence-specific ^{13}C and ^{15}N assignments are discussed in the following paper (Wang et al., 1990). The spin systems of several long-chain amino acids remain to be assigned; nevertheless, we have been able to achieve almost total assignments of three α-helical domains and the domains of three antiparallel β-pleated sheets with reverse turns. Detailed determination of the secondary structure of the nuclease H124L ternary complex in solution permits a comparison with the structure in the crystalline state and provides a starting point for studies of conformational alterations caused by changes in solution properties or by changes in the amino acid sequnce of the protein.

Experimental Procedures

Plasmid Construction. The *Hin*dIII restriction site of the T7 RNA polymerase expression vector pET3A (Rosenberg et al., 1987) was excised by digestion with *Eco*RI and *Eco*RV, followed by end-filling with Klenow fragment and ligation. The plasmid copy control region was removed by a *Pvu*II/*Bgl*II digest, end-filling, and ligation. In order to insert the nuclease gene, the *Bam*HI site directly downstream of the T7 promoter was cleaved, end-filled, and blunt-end ligated to a *Bgl*II linker. The *Nde*I–*Sau*3A fragment containing the wild-type staphylococcal nuclease gene (Shortle & Meeker, 1989) was cloned into the *Nde*I and *Bgl*II sites to generate pTSN1. The regenerated *Bgl*II site allowed us to clone in the downstream sequence of the H124L gene between the *Hin*dIII and *Bgl*II sites of pTSN1 so as to generate the pET3A-H124L derivative pTSN2.

Protein Samples. Nuclease H124L at natural isotopic abundance was isolated from *Escherichia coli* which contained plasmid Z101 provided by Dr. Shortle (Shortle & Lin, 1985). Cell culture and protein isolation were as described previously (Alexandrescu et al., 1988). The growth medium and growth conditions for production of the random fractionally deuterated sample were carried out as described previously (LeMaster & Richards, 1988) with the variations that the level of deuteration in H_2O and carbon sources was approximately 55% and that BL21 (DE3) (Studier & Moffatt, 1986) was used as the bacterial host. The cells were induced at 0.8 OD_{600} with 120 mg/L of isopropyl β-D-thiogalactopyranoside and harvested after 3 h. The yield of deuterated protein was 350 mg for 6 mL.

Sample Preparation for NMR Spectroscopy. Protein samples used for NMR experiments in ^2H_2O were dissolved in 100% ^2H_2O, and all labile protons were exchanged fully for deuterons by heating the sample at 45 °C for 1 h. For experiments in H_2O, the protein was dissolved in 90% H_2O/10% ^2H_2O. Two complexes were studied (dissolved in H_2O or in ^2H_2O as noted): (a) The complex containing natural abundance nuclease H124L, [na]H124L-TC. These samples consisted of 3.5 mM protein, 10.5 mM pdTp, 21 mM $CaCl_2$, and 0.3 M KCl. (b) The complex containing 50% random fractionally deuterated nuclease H124L, [50% ul ^2H]-H124L-TC. These samples consisted of 5 mM protein, 15 mM pdTp, 30 mM $CaCl_2$, and 0.3 M KCl. The pH was adjusted to a meter reading of 5.5 for ^2H_2O solutions and of 5.1 for H_2O solutions.

NMR Spectroscopy. NMR spectra were acquired with Bruker AM-500 or AM-600 spectrometers at a temperature setting of 45 °C. ^1H chemical shifts are reported relative to that of internal TSP (at 0 ppm). Two-dimensional NMR spectra were calibrated by assigning the clearly resolved cross peak of the ribose $C_1{}'H$ of pdTp a chemical shift value of 6.3 ppm relative to internal TSP.

Two-dimensional, phase-sensitive, double-quantum filtered $^1H\{^1H\}$ correlated spectra (DQF-COSY) (Rance et al., 1983) were acquired with the D_1–90°–D_0–90°–D_3–90°–Acq pulse sequence, where D_1 is the relaxation delay time and Acq is the acquisition period. Phase-sensitive $^1H\{^1H\}$ correlated spectra (COSY) (Marion et al., 1983) were acquired with the D_1–90°–D_0–90°–Acq pulse sequence. DQF-COSY data were recorded with [na]H124L-TC and [50% ul ^2H]H124L-TC in ^2H_2O, and phase-sensitive COSY data were recorded with [50% ul ^2H]H124L-TC in H_2O. Data from the AM-500 spectrometer were collected for 512 values of t_1, and 4096 points were collected in t_2. Double zero-filling was used to extend the t_1 dimension. Shifted sine bell window functions were applied in both dimensions to spectra recorded in ^2H_2O for resolution enhancement.

Two-dimensional $^1H\{^1H\}$ NOE spectra (NOESY) (Anil Kumar et al., 1980; Bodenhausen et al., 1984) were acquired at 500 and 600 MHz with the D_1–90°–D_0–90°–τ_m–90°–Acq pulse sequence, where τ_m is the mixing time during which the NOE builds up. Scalar correlation effects were eliminated by random variation of τ_m (Macura et al., 1982). NOESY data were collected with samples dissolved in ^2H_2O and H_2O at the following mixing times: τ_m = 100, 150, and 200 ms for

[2] The amino terminus of the protein is disordered in the X-ray structure and is not essential for enzymatic activity.

[na]H124L-TC and 250 ms for [50% ul ^{2}H]H124L-TC. Acquisition parameters and data (^2H_2O) processing parameters for 500-MHz spectra were identical with those given in COSY experiments. The Gaussian weighting function was used in both dimensions for data recorded in H_2O.

Two-dimensional ^{1}H{^{1}H} Hartmann–Hahn magnetization transfer (HOHAHA) spectra (Bax & Davis, 1985) were acquired with the D_1–90°–D_0–SL_x–MLEV-17–SL_x–Acq pulse sequence, where SL_x denotes a short (2 ms) spin-lock field applied along the x axis and MLEV-17 is a composite pulse sequence repeated N times. HOHAHA spectra were recorded at spin-lock mixing times of 55 and 75 ms with [na]H124L-TC dissolved in ^2H_2O. The acquisition parameters were identical with those given above for COSY experiments.

Two-dimensional phase-sensitive ^{1}H{^{1}H} relayed coherence transfer spectra (RCT-COSY) (Wagner 1983; Bax & Drobny, 1985) were acquired with the D_1–90°–D_0–90°–D_2–180°–D_2–90°–Acq pulse sequence, where D_2 is the mixing time. RCT-COSY data were recorded at 500 MHz with [50% ul ^{2}H]H124L-TC dissolved in H_2O at mixing times of 30, 45, and 58 ms.

Results and Discussion

Assignment Strategy. The DQF-COSY spectrum of [na]H124L-TC in ^2H_2O showed regions of heavy overlap and lacked numerous expected connectivities, especially in the ^{1}H aliphatic region. The overlap problem was not overcome even with the complex containing random fractionally deuterated nuclease ([50% uL ^{2}H]H124L-TC). Therefore, we found the standard method of sequential assignment (Billeter et al., 1982; Wüthrich, 1986) difficult to apply to the nuclease ternary complex.

The strategy used here for identifying secondary structure involved the unequivocal determination of stretches of $^1H^N$–$^1H^N$ and $^1H^\alpha$–$^1H^N$ connectivities in NOESY spectra obtained in H_2O. These were then extended to the fingerprint region of the COSY spectrum in H_2O where $^1H^\alpha$–$^1H^N$ connectivities of Ala, Val, Thr, Gly, and other spin systems had been located by preliminary spin system assignments on the basis of COSY, HOHAHA, and RCT-COSY experiments. Specific assignments for α-helices and β-pleated sheets could then be based on the uniqueness in the protein sequence of sequentially related stretches containing the assigned residues (Cusumano et al., 1968; Shortle, 1983). The assignments were then extended to other spin systems in α-helix and β-sheet domains by cross-checking sequential assignments against spin system identification (Wüthrich, 1986). Identifications of amino acid types at this stage were based partially on RCT-COSY (H_2O) and partially on NOESY (H_2O) by predicting intraresidue $^1H^\alpha$–$^1H^N$ and $^1H^\beta$–$^1H^N$ NOE's from $^1H^\alpha$–$^1H^\beta$ cross peaks in the COSY spectrum (^2H_2O). The resulting assignments were confirmed and extended by heteronuclear 2D NMR experiments (Wang et al., 1990).

Identification of the ^{1}H Spin Systems of Thr, Ala, Val, Gly, Ser, and Ile. ^{1}H NMR spin system identification relied primarily on delineation of the cross peak patterns (Wüthrich, 1986) in HOHAHA, COSY, and RCT-COSY spectra, with additional evidence from qualitative analysis of the COSY cross peak multiplet fine structures (Neuhaus, 1985; Wüthrich, 1986). The spin system assignments of Thr, Ala, and Val are documented in the ^{1}H HOHAHA spectrum of [na]H124L-TC in ^2H_2O (Figure 1). The relevant cross peaks are indicated with the one-letter code for the amino acid type and an arbitrary number. Relayed cross peaks are denoted by asterisks. Nine of the ten Thr spin systems were identified from $^1H^\alpha$–$(^1H^\gamma)_3$ relayed cross peaks as shown in Figure 1A. The

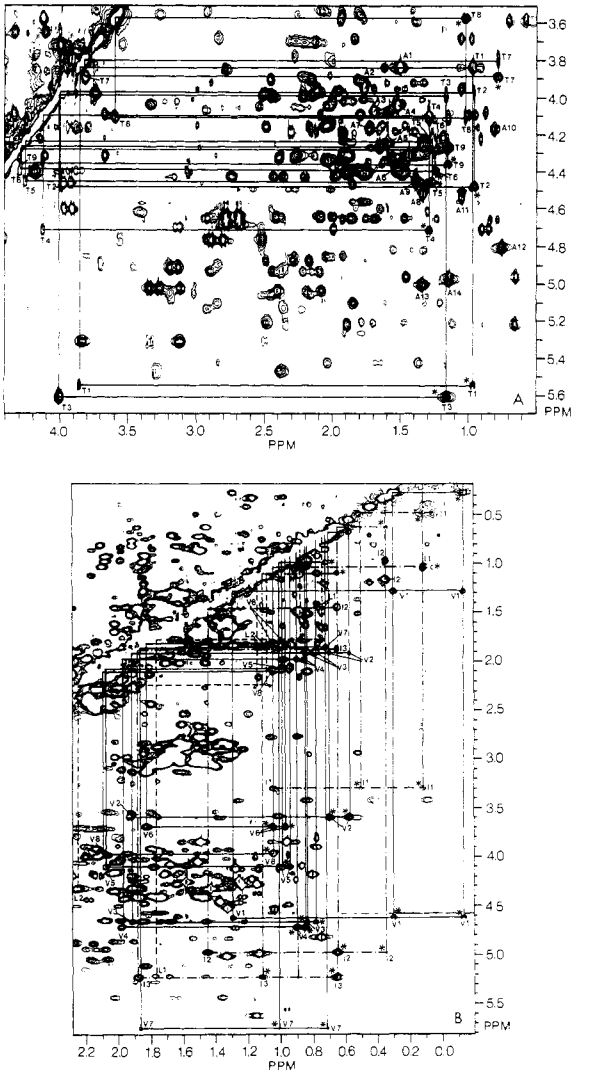

FIGURE 1: Portions of the 600-MHz HOHAHA spectrum of [na]-H124L-TC in ^2H_2O solution. The spectrum was recorded with 600 values in t_1 and 120 scans for each t_1 value. Cross peaks identified with particular amino acids are indicated by the one-letter code with an arbitrary number. (*A*) Region containing spin systems assigned to Thr (continuous lines) and Ala. Hartmann–Hahn relay cross peaks are denoted by asterisks. (B) Region containing spin systems assigned to Val (continuous lines), Leu (broken lines), and Ile (dashed-dotted lines).

tenth Thr spin system was identified by a heteronuclear 2D experiment (Wang et al., 1990).

The $^1H^\alpha$–$^1H^\beta$ cross peaks from all 14 Ala residues are identified in Figure 1A. Alanine spin systems were distinguished from those of threonine by their lack of $^1H^\beta$–$(^1H^\gamma)_3$ relayed cross peaks in HOHAHA spectra (^2H_2O). The assignments were confirmed by a ^{1}H{^{13}C} multiple-bond correlation experiment (Wang et al., 1990).

Valine residues give rise to unique RCT-COSY cross peak patterns which contain $^1H^\alpha$–$(^1H^{\gamma_1})_3$, $^1H^\alpha$–$(^1H^{\gamma_2})_3$, and $(^1H^{\gamma_1})_3$–$(^1H^{\gamma_2})_3$ connectivities. Complete patterns of this type were found for seven of the nine Val residues (Figure 1B). One of the remaining Val residues has degenerate chemical shifts for $(^1H^{\gamma_1})_3$ and $(^1H^{\gamma_2})_3$ and thus shows only a single relayed peak at 1.05,3.94 ppm. Figure 1B shows another pair of cross peaks at 0.89,2.18 and 1.15,2.18 ppm, one of which has a relayed peak at 0.89,1.13 ppm but has no $^1H^\alpha$–$(^1H^{\gamma_1})_3$ or $^1H^\alpha$–$(^1H^{\gamma_2})_3$ relayed cross peaks. A ^{1}H{^{15}N}SBC-NOE experiment, however, revealed that they should be assigned to Val (Wang et al., 1990).

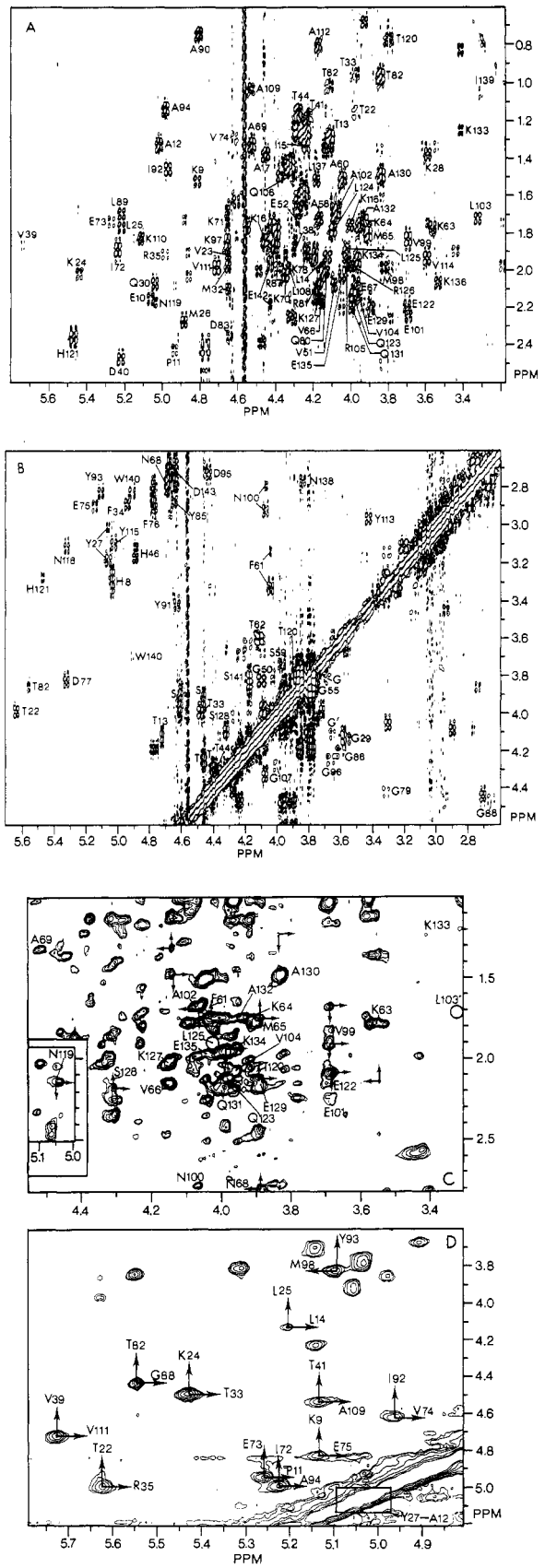

FIGURE 2: Aliphatic regions of two-dimensional 500-MHz NMR spectra of [50% ul ^2H]H124L-TC in ^2H_2O solution. Spectra were recorded with a 6500-Hz spectral width, and a total 128 scans was accumulated for each t_1 value. 750 increments were collected. Zero-filling was applied in t_1 to extend it to 4096 points. Assigned cross peaks are labeled with the one-letter amino acid code and residue number. (A and B) Regions of the phase-sensitive DQF-COSY spectrum. (C and D) Regions of the NOESY spectrum collected with a 250-ms mixing time. COSY-type cross peaks are circled.

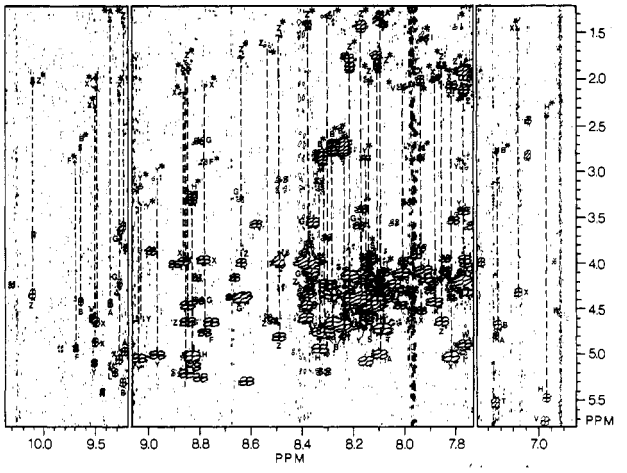

FIGURE 3: 500-MHz relayed-COSY spectrum of [50% ul ^2H]-H124L-TC in H_2O solution. The spectrum was recorded with 600 increments and 160 scans for each t_1 value. The mixing time was set to 45 ms. See text for explanation of cross peaks. Relayed cross peaks are denoted by asterisks.

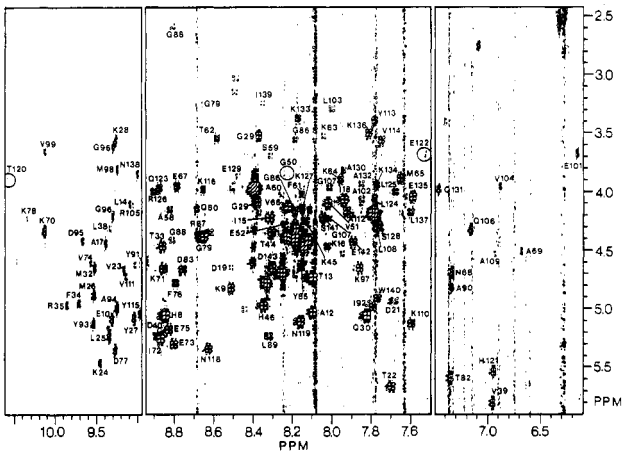

FIGURE 4: Fingerprint region of 600-MHz phase-sensitive COSY spectrum of [50% ul ^2H]H124L-TC in H_2O solution. The spectrum was recorded with a 7462-Hz spectral width, and a total of 132 scans were accumulated for each t_1 value. 700 increments were collected. Zero-filling was applied to t_1 to extend it to 4096 points. Assigned cross peaks are indicated by the one-letter amino acid code with sequence numbers.

The glycine spin system typically has a unique COSY pattern of fine structure located in the range between 2.6 and 4.5 ppm. Six of the ten Gly residues of the ternary complex can be identified on this basis (Figure 2B). In addition, Gly residues give unique RCT-COSY cross peaks between the $^1H^N$ and the two $^1H^\alpha$ nuclei. Two additional Gly spin systems could be identified on this basis in the RCT-COSY spectrum (Figure 3) and the fingerprint region of the COSY spectrum (Figure 4), both recorded in H_2O. The remaining two Gly residues were assigned by reference to $^1H\{^{13}C\}$SBC data (Wang et al., 1990).

Inspection of the COSY spectrum (Figure 2B) around 4 ppm reveals standard patterns for three of the five Ser spin systems in which the $^1H^{\beta_1}$ and $^1H^{\beta_2}$ chemical shifts are non-degenerate and show small geminal coupling, $^3J_{\beta\beta'}$. The remaining two Ser residues may have degenerate $^1H^{\beta_1}$ and $^1H^{\beta_2}$ chemical shifts and exhibit complex peaks. This was shown also by a $^1H\{^{15}N\}$SBC-NOE experiment (Wang et al., 1990).

Among the 10 different COSY connectivity patterns for aliphatic protons (Wüthrich, 1986), only the δ-methyl group of Ile gives cross peaks to two γ_1-protons. By use of these $(^1H^\delta)_3$–$^1H^{\gamma_1}$ cross peaks as starting points, the $^1H^\alpha$–$^1H^\beta$ direct

cross peaks, the $^1H^{\alpha}$–$^1H^{\gamma_1}$, $^1H^{\alpha}$–$^1H^{\gamma_1}$, and $^1H^{\alpha}$–$(^1H^{\gamma_2})_3$ relayed cross peaks, and the $^1H^{\alpha}$–$(^1H^{\delta})_3$ double-relayed cross peaks of three of the five Ile residues could be found in the HOHAHA spectrum (Figure 1B). The connectivities of I1 and I2 are easily spotted. The I3 spin system was easily distinguished by extending a $(^1H^{\gamma_2})_3$–$^1H^{\beta}$ connectivity at 0.66,1.9 ppm to the $^1H^{\alpha}$ region. The above assignments were confirmed by a $^1H\{^{13}C\}$SBC-NOE experiment which also established the assignments of the other two Ile residues (Wang et al., 1990).

Nuclease H124L contains 12 Leu residues. Although pairs of Val $^1H^{\beta}$–$(^1H^{\gamma})_3$ and Leu $^1H^{\gamma}$–$(^1H^{\delta})_3$ connectivities appear in the same region, $^1H^{\beta}$–$(^1H^{\delta})_3$ relayed cross peaks appear only for Leu and serve to identify this residue. Spin systems for L1 and L2 have been identified in this way (Figure 1B). Spin systems of several additional Leu residues were identified by ^1H–^{15}N 2D experiments with [98% ^{15}N]Leu-H124L-TC (Wang et al., 1990).

Extension of Identified ^1H Spin Systems to Backbone Amide Protons. At the contour level of Figure 4, the fingerprint region of the COSY spectrum of [50% ul ^2H]-H124L-TC shows cross peaks from 141 of the 149 amino acid residues of the protein (no cross peaks are expected for the six prolines, and two peaks are observed for five of the ten glycines). At lower contour levels, cross peaks from three additional amino acid residues are visible as indicated by circles in Figure 4.

In the two spectral regions bounded by (ω_1 = 4.7–5.8 ppm, ω_2 = 6.9–10.2 ppm) and (ω_1 = 3.3–3.7 ppm, ω_2 = 6.9–10.2 ppm) (Figure 4), the $^1H^N$–$^1H^{\alpha}$ connectivities are sufficiently well dispersed so that they can be matched up with the subset of $^1H^N$–$^1H^{\alpha}$ cross peaks that appear in the COSY spectrum of the complex recorded in ^2H_2O (Figure 2A,B). Each of these peaks is easily connected to the rest of its spin system. This led to fingerprint region assignments for three Ala, four Val, four Thr, three Ile, one Leu, five Gly, and several aromatic residues (Figure 4).

Additional assignments of fingerprint region $^1H^N$–$^1H^{\alpha}$ cross peaks were made by the combined analysis of COSY and RCT-COSY spectra recorded in H_2O. The amino acid residues Tyr, Phe, His, Trp, Asp, and Asn have fine structure patterns characteristic of AMX spin systems: no $^1H^{\gamma}$ and usually nondegenerate chemical shifts for the two $^1H^{\beta}$ nuclei. The random coil $^1H^{\beta}$ chemical shifts of these residues lie in the 2.75–3.9 ppm range (Bundi et al., 1979). In the RCT-COSY spectrum of [50% ul ^2H]H124L-TC (Figure 3), the relayed $^1H^N$–$^1H^{\beta}$ cross peaks with $^1H^{\beta}$ downfield of 2.7 ppm were relegated to this group of amino acid residues. Identifications according to individual kinds of aromatic amino acids were based on connectivities observed in NOESY spectra (^2H_2O) (not shown) between $^1H^{\beta}$ resonances and certain aromatic ring protons or on $^1H\{^{13}C\}$SBC-NOE data (Wang et al., 1990). Resonances of 10 of the 14 aromatic residues are given in Figure 3. The remaining five AMX spin systems having $^1H^{\beta}$ resonances in the 2.7–3.4 ppm region were identified as Asp and Asn. Ser and Thr residues are expected to contribute relayed cross peaks with $^1H^{\beta}$ downfield of 3.7 ppm (Bundi et al., 1979). However, only a few relayed cross peaks from Ser and Thr appeared in this region as indicated in Figure 3.

Fingerprint region cross peaks of amino acid residues with methyl protons can be identified in single or double RCT-COSY spectra if connectivities between the $^1H^N$ and the methyl protons can be established. Similarly, single and double RCT-COSY spectra, in principle, can be used to identify amino acid residues with long side chains provided that $^1H^N$–$^1H^{\beta}$ and $^1H^N$–$^1H^{\gamma}$ connectivities can be established. However, the efficiency of relayed coherence transfer depends critically on the spin–spin coupling constants and the transverse relaxation time T_2 (Chazin, 1987). The slow tumbling of staphylococcal nuclease (M_r 17 000) leads to a short T_2, and since about 88 of the 149 residues are expected to be involved in α-helix, β-sheet, or reverse turns (Cotton et al., 1979), a wide range of $^1H^N$–$^1H^{\alpha}$ spin–spin coupling constants is expected. These factors lead to cancellation of cross-peak intensity in single or double RCT-COSY experiments and make it difficult, at this stage, to use these experiments to obtain additional spin system assignments in the fingerprint region.

By use of a combination of COSY spectra recorded in H_2O and ^2H_2O and the NOESY spectrum recorded in H_2O, the fingerprint region COSY cross peaks can be classified into several groups: Asp and Asn denoted as B, Glu, Gln, and Met as X, and Leu, Ile, Lys, and Arg as Z. The random coil chemical shifts of the $^1H^{\beta}$ nuclei of Glu, Gln, Met, and Val residues are around 2.0–2.6 ppm, while those of Leu, Ile, Lys, and Arg residues are around 1.5–2.0 ppm. Alanine $(^1H^{\beta})_3$ chemical shifts normally appear upfield of other methyl groups (Bundi et al., 1979). These characteristic were used to classify $^1H^N$–$^1H^{\alpha}$ and $^1H^N$–$^1H^{\beta}$ cross peaks in the NOESY (H_2O) spectrum and $^1H^{\alpha}$–$^1H^{\beta}$ cross peaks in the COSY (^2H_2O) spectrum. Chemical shifts from $^1H^{\alpha}$–$^1H^{\beta}$ COSY (^2H_2O) cross peaks were used to search for intraresidue cross peaks in the NOESY (H_2O) spectrum. This approach led to a rough classification of peaks in the fingerprint region according to amino acid type. The rigorous identifications were obtained only after the sequential assignments were made.

Determination of Three α-Helical Domains. An α-helix is characterized by a continuous stretch of strong sequential d_{NN} NOE's and medium-range $d_{\alpha N}(i,i+3)$ and $d_{\alpha\beta}(i,i+3)$ NOE's. Furthermore, weak $d_{NN}(i,i+2)$ NOE's may be detected along part of the α-helix (Wagner et al., 1986). NOESY spectra of the ternary complex (H124L-TC) acquired in H_2O were searched for sequential d_{NN} connectivities and characteristic nonsequential NOE's. NOESY spectra of the ternary complex acquired in ^2H_2O were searched for $d_{\alpha\beta}(i,i+3)$ NOE's. Three long stretches of sequential d_{NN} connectivities were identified. Figure 5 shows a summary of the NOE's used to determine α-helical domains. Table I gives the chemical shifts of assigned cross peaks.

(1) α-Helix from Ala^{58} to Ala^{69}. The complete set of sequential $d_{\alpha N}$ NOE's from an α-helix sometimes is difficult to detect. Thus, the $d_{\alpha N}$ connectivities for residues 58–69 are broken into shorter segments as shown in Figure 6A. These $d_{\alpha N}$ connectivities confirm several steps in the d_{NN} sequential walk (Figure 6B). Since $d_{\alpha N}$ connectivities are directional, they establish the polarity of the d_{NN} sequential walk as indicated by arrows in Figure 6B. The $d_{NN}(i,i+2)$ NOE's are indicated by arrows pointing to positions of corresponding residues in the peptide segment (Figure 6B). The assignment of this long segment as a helical domain was also confirmed by the observation of $d_{\alpha N}(i,i+3)$ and $d_{\alpha\beta}(i,i+3)$ connectivities. The $d_{\alpha N}(i,i+3)$ NOE's are indicated by arrows pointing to the $^1H^{\alpha}$ and $^1H^N$ positions of corresponding cross peaks in the fingerprint region (Figure 6A). The $d_{\alpha\beta}(i,i+3)$ NOE's also support the characterization of this segment as α-helix (Figure 2C).

Three alanine residues were found to be involved in this α-helical segment: in positions 1, 3, and 12. This pattern of alanines is unique in the protein sequence (Figure 5) and assigns this helix to Ala^{58}–Ala^{69}, as was confirmed by the presence of additional spin systems in this helical stretch whose

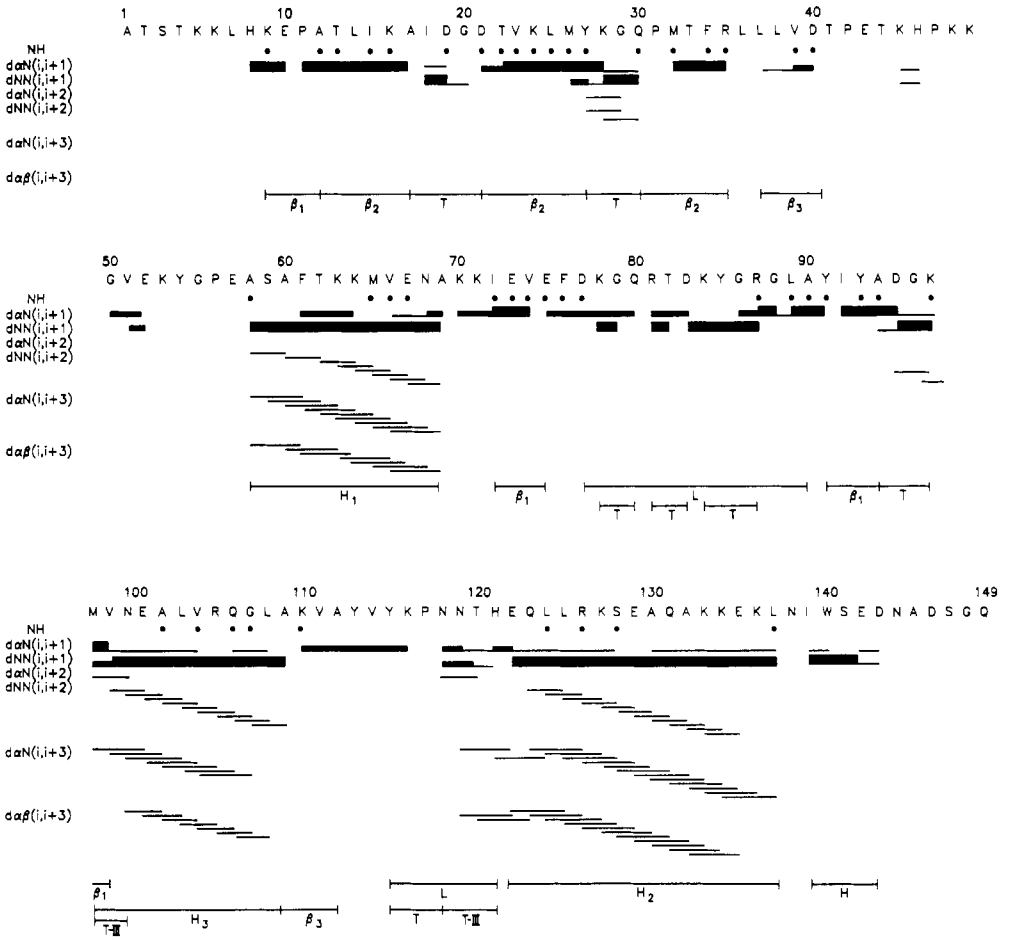

FIGURE 5: Amino acid sequence of nuclease H124L with a summary of information derived from the NMR experiments on its ternary complex (H124L-TC). Sequential $d_{\alpha N}$ and d_{NN} NOE connectivities and $d_{\alpha N}(i,i+2)$, $d_{NN}(i,i+2)$, $d_{\alpha N}(i,i+3)$, and $d_{\alpha\beta}(i,i+3)$ connectivities are indicated by bars. Slowly exchanging amides are indicated by filled circles. Locations of secondary structural elements as deduced from the present NMR results are indicated by bars and symbols: H, α-helix; T-III, type III reverse turn; T, turn; L, loop; β, antiparallel β-sheet.

patterns agreed with the sequence Ser[59], Phe[61], Val[66], and Thr[62]. Spin systems of the remaining residues in this stretch were then assigned to Lys[63], Lys[64], Met[65], Glu[67], and Asn[68]. Heteronuclear ^1H–^{13}C and ^1H–^{15}N 2D NMR experiments (Wang et al., 1990) confirmed the latter assignments.

(2) α-Helix from Glu[122] to Leu[137]. A second helix was deduced from $d_{\alpha N}$ connectivities (Figure 7A) and corresponding d_{NN} connectivities (Figure 7B). The sequential d_{NN} walk, which starts at ω_2 = 7.54 ppm and ends at ω_2 = 7.61 ppm, involves 16 amino acid residues. The $d_{NN}(i,i+2)$ connectivities could be identified throughout the long sequence as indicated in Figure 7B. The $d_{\alpha N}(i,i+3)$ NOE's (Figure 7A) and the $d_{\alpha\beta}(i,i+3)$ NOE's (Figure 2C) confirm the characterization of this stretch as α-helix.

The corresponding fingerprint region COSY cross peaks (Figure 7A) show that this stretch contains an A-X-A tripeptide. Two such tripeptides are found in the nuclease H124L sequence: Ala[58]-Ser[59]-Ala[60] and Ala[130]-Gln[131]-Ala[132]. Since the former tripeptide is contained in the helix assigned above, the present long sequence is assigned to Glu[122]–Leu[137].

In addition to the two alanine residues, peptide segment Glu[122]–Leu[137] (Figure 5) contains eight Z-type residues, five X-type residues, and one serine residue. Sequential assignments of the spin systems that comprise this segment, as built up from $^1H^N$–$^1H^N$ and $^1H^\alpha$–$^1H^N$ connectivities, led to ordering of identified spin systems (Figure 3) in agreement with the sequence. Specific assignments of Lys, Arg, and Leu were confirmed by heteronuclear experiments carried out with ternary complexes made with nuclease H124L labeled in these residues with ^{13}C or ^{15}N (Wang et al., 1990).

(3) α-Helix from Met[98] to Ala[109]. The third long sequence of 12 residues was identified from $d_{\alpha N}$ (Figure 8A) and d_{NN} connectivities (Figure 8B). The $d_{\alpha N}$ conectivities established the direction of the d_{NN} sequential walk (Figure 8B) from a cross peak at ω_2 = 9.24 ppm to a cross peak at ω_2 = 6.93 ppm. The observed $d_{NN}(i,i+2)$, $d_{\alpha N}(i,i+3)$, and $d_{\alpha\beta}(i,i+3)$ NOE's (Figures 2C and 8) support the identification of this stretch as α-helical. As shown by extension of the $^1H^N$ chemical shifts of the residues contained in this peptide segment (Figure 8B) to fingerprint region cross peaks (Figure 8A), two valine residues occupy the second and seventh positions, two alanines occupy the fifth and twelfth positions, and one glycine occupies the tenth position. These constraints locate this segment uniquely within the sequence (Figure 5) to Met[98]–Ala[109]. The medium-range NOE observed between the $^1H^N$ protons of Met[98] and Val[99] suggests that the beginning of the α-helix is distorted.

The cross peak expected from Asn[100] is missing in the COSY (H_2O) fingerprint region (Figure 4). However, the position of the cross peak can be predicted from $d_{\alpha N}$ connectivities (Figure 8A). The NOESY cross peak at 9.58,3.68 ppm corresponds to the $d_{\alpha N}(i-1,i)$ NOE cross peak between residues Val[99] and Asn[100] (Figure 8A), and the NOESY cross peak at 6.16,4.07 ppm corresponds to a $d_{\alpha N}(i,i+1)$ NOE between residues Glu[101] and Asn[100]. Therefore, the fingerprint region cross peak of residue Asn[100] should be located at 9.58,4.07 ppm. The $d_{\alpha N}$ connectivity between Asn[100] and Glu[101] was confirmed by a $^1H\{^{15}N\}$SBC-NOE experiment, and assign-

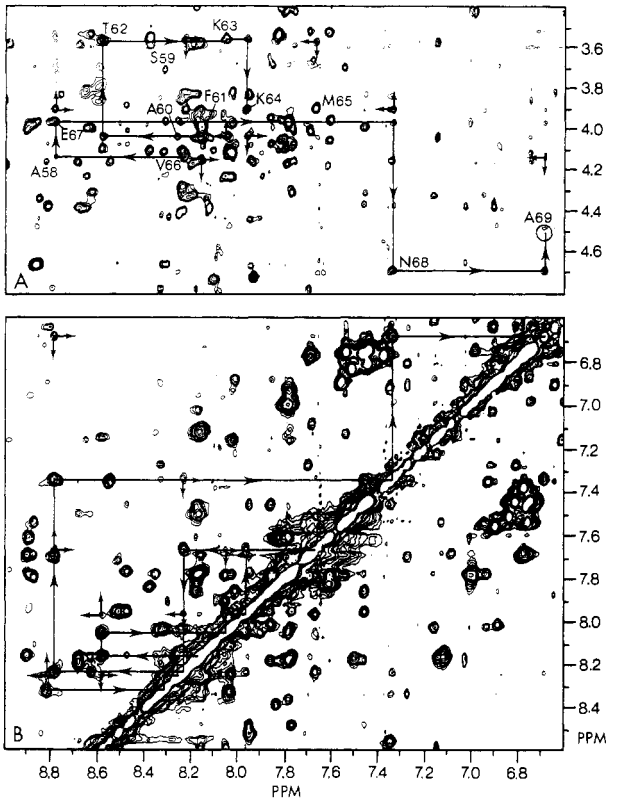

FIGURE 6: Evidence for an α-helix running from Ala[58] to Ala[69] from portions of the 600-MHz NOESY spectrum of [50% ul ^{2}H]H124L-TC in H_2O solution. The spectrum was recorded with 700 values in t_1 and with 132 scans for each t_1 value. Zero-filling was applied to t_1 in order to extend it to 4096 points. (A) Weak sequential $d_{\alpha N}$ connectivities of the helix are indicated by solid lines. The spectral positions of corresponding COSY cross peaks are circled. (B) Long sequential d_{NN} connectivities are traced by the solid line. Nonsequential $d_{\alpha N}(i,i+3)$ and $d_{NN}(i,i+2)$ NOE's that arise from the helical repeat are indicated by arrows at right angles.

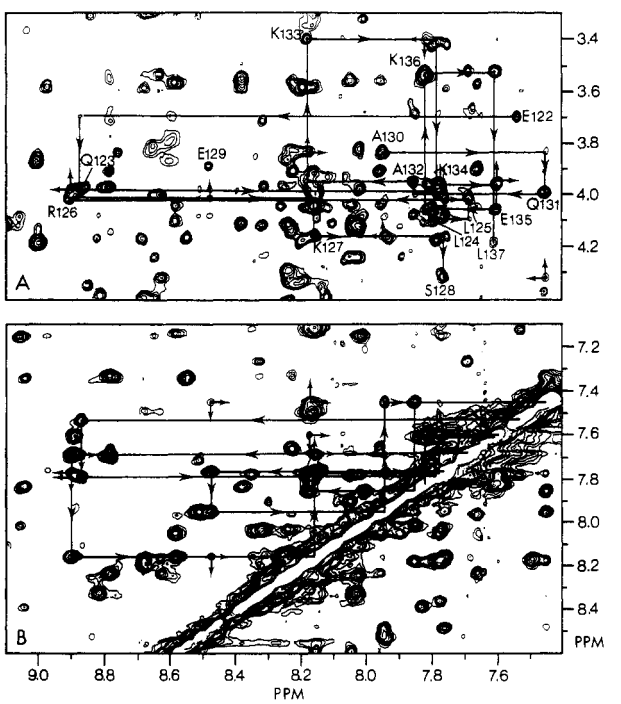

FIGURE 7: Evidence for an α-helix running from Glu[122] to Leu[137]. (A) Partial $d_{\alpha N}$ NOE connectivities in the helix are indicated. The corresponding fingerprint region cross peaks are indicated by circled regions. (B) The sequential backbone amide proton connectivities are indicated by continuous lines. The nonsequential NOE $d_{NN}(i,i+2)$ and $d_{\alpha N}(i,i+3)$ connectivities are indicated by arrows at right angles.

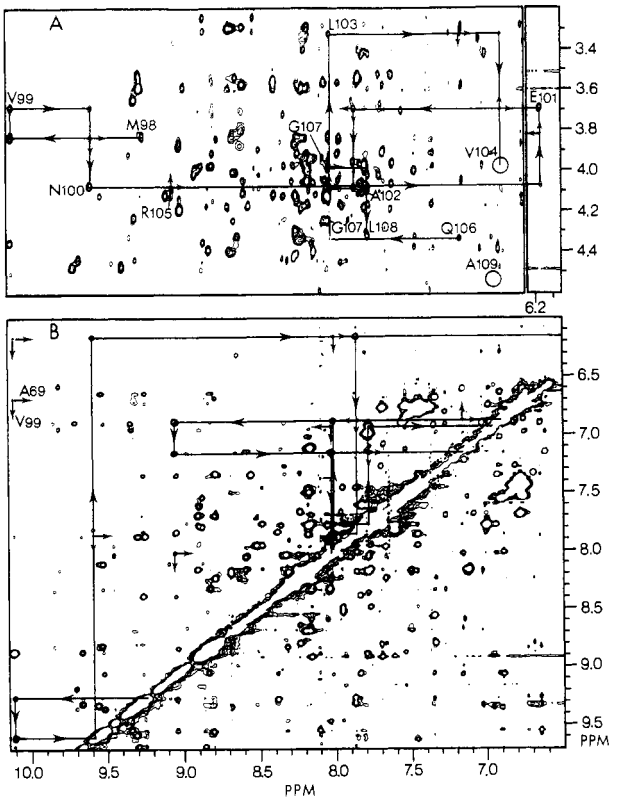

FIGURE 8: Evidence for an α-helix running from Met[98] to Ala[109]. (A) Sequential $d_{\alpha N}$ walk. The circled regions denote the corresponding fingerprint region COSY cross peaks. (B) Sequential d_{NN} walk from residues Met[98] to residue Ala[109]. Nonsequential NOE's are indicated by arrows at right angles.

ments of Met[98], Glu[101], Leu[103], Leu[103], Arg[105], and Asn[106] were confirmed by ^{1}H{^{15}N} heteronuclear experiments (Wang et al., 1990).

The NOE cross peak at 9.58,3.82 ppm (Figure 8A) corresponds to a $d_{\alpha N}(i,i+2)$ connectivity between the $^1H^{\alpha}$ of Met[98] and the $^1H^N$ of Asn[100]. This NOE indicates (Wagner et al., 1986) that the segment Met[98]-Val-[99]-Asn-[100] forms a type III reverse turn. The fact that residues Met[98] and Val[99] also are involved in a β-sheet (see below) may explain the presence of this type III reverse turn at the beginning of an α-helix.

Determination of Antiparallel β-Pleated Sheet and Turns. Antiparallel β-sheet structure gives rise to a characteristic pattern of strong, sequential $^1H^{\alpha}$–$^1H^N$ NOE connectivities as well as to strong NOE's between $^1H^{\alpha}$ protons of opposite strands. In addition, several typical NOE's are expected between protons of opposite strands of antiparallel β-sheet: namely, $d_{\alpha N}(i,j+1)$ or $d_{\alpha N}(j,i+1)$ and $d_{NN}(i-1,j+1)$ or $d_{NN}(i+1,j-1)$. Observation of all these NOE cross peaks reveals the existence of antiparallel β-sheet (Englander, 1987).

The four major classes of reverse turn (Richardson, 1981) can be identified from NOE patterns (Wagner et al., 1986). Within a reverse turn, one expects to observe one or two steps of sequential $d_{\alpha N}$ and d_{NN} connectivities; $d_{\alpha N}(i,i+2)$ and $d_{NN}(i,i+2)$ connectivities also provide evidence for such a structure. For a type II turn, the local conformation usually requires a glycine at residue $i + 2$.

The $^1H^{\alpha}$–$^1H^N$ and $^1H^N$–$^1H^N$ connectivitiy regions of the NOESY (H_2O) spectrum were searched for connectivities characteristic of β-sheet and reverse turns, and the NOESY (^2H_2O) spectrum was searched for $^1H^{\alpha}$–$^1H^{\alpha}$ NOE's. Three antiparallel β-sheets with three reverse turns were identified. Chemical shifts of residues involved in these structures are summarized in Table I.

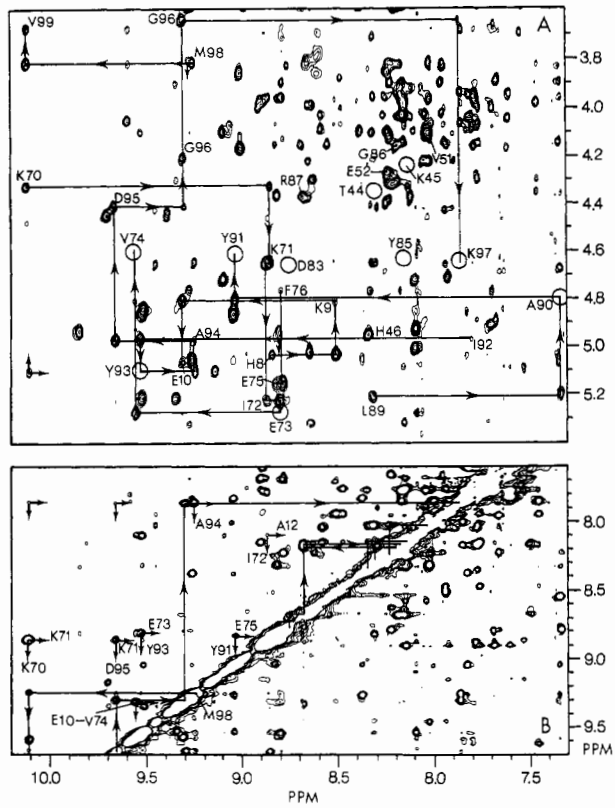

FIGURE 9: Determination of antiparallel β-sheet and turns involving segments Lys[9]–Ala[12], Ile[72]–Glu[75], and Tyr[91]–Val[99]. The long-range NOE $d_{NN}(i,i+2)$ and $d_{\alpha N}(i,i+3)$ connectivities are indicated. (A) Strong $d_{\alpha N}$ sequential connectivities of the β-sheet. The corresponding COSY cross peaks in the fingerprint region are circled. (B) A short d_{NN} sequential walk, from Asp[95] to Lys[97], which illustrates the reverse turn observed in this β-sheet.

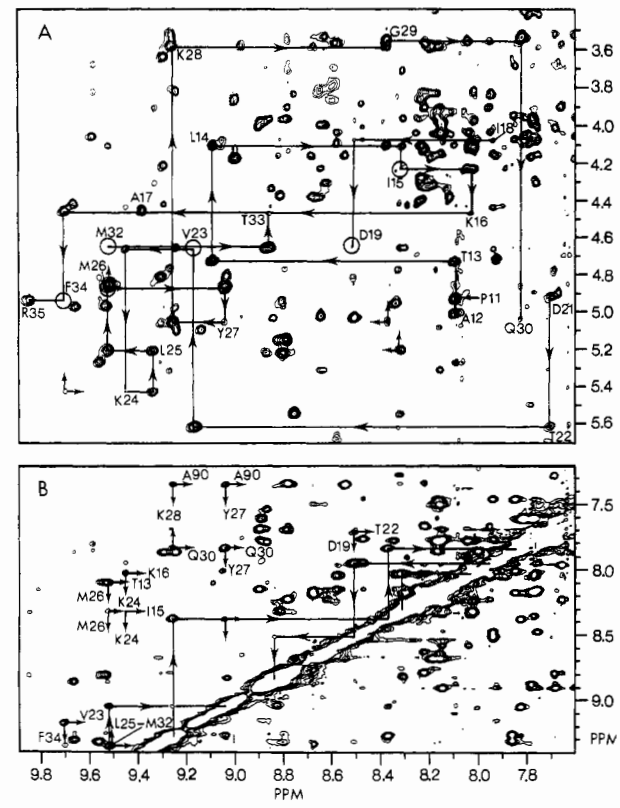

FIGURE 10: Evidence for antiparallel β-sheet containing the segment Ala[12]–Arg[35]. (A) The $d_{\alpha N}$ sequential walk. Corresponding COSY cross peaks are circled. (B) The d_{NN} sequential connectivities which reveal the reverse turns in this β-sheet. All observed long-range NOE connectivities within this β-sheet are indicated by arrows at right angles.

(1) Antiparallel β-Sheet and Turn Involving Segments Lys[9]–Ala[12], Ile[72]–Glu[75], and Tyr[91]–Val[99]. Several peptide segments with strong $d_{\alpha N}$ sequential connectivities were located in Figure 9A. One hexapeptide and one tripeptide were assigned to Ile[92]–Lys[97] and Leu[89]–Tyr[91] on the basis of the unique sequences I-Y-A and Z-A-Y (Figure 5). The $d_{\alpha N}$ NOE's of segment Asp[95]–Lys[97] are weak. An interstrand NOE was observed between the $^1H^{\alpha}$ of Tyr[93] and the $^1H^N$ of Val[99]; similarly, an interstrand NOE was observed between the $^1H^{\alpha}$ of Met[98] and the $^1H^N$ of Ala[94] (Figure 9A). Furthermore, the observed strong $^1H^N$–$^1H^N$ NOE between Ala[94] and Lys[97] (Figure 9B) and $^1H^{\alpha}$–$^1H^{\alpha}$ NOE between Tyr[93] and Met[98] residues (Figure 2D) suggest that the Met[98]-Val[99] and Ile[92]-Tyr[93]-Ala[94] peptide segments should be located in two adjacent strands of one antiparallel β-sheet.

A short sequential walk of strong d_{NN} connectivities was distinguished as a segment of three residues (Figure 9B). The d_{NN} NOE's between Asp[95]-Gly[96] and Gly[96]-Lys[97] are strong, and that between Asp[95] and Lys[97] is weak (Figure 9B). This observed pattern of NOE's provides evidence (Wagner et al., 1986) that segment Ala[94]–Lys[97] forms a type I reverse turn.

A four-step sequential $d_{\alpha N}$ walk (Figure 9A) defines a segment containing the tripeptide I-X-V. Since the amino acid sequence (Figure 5) contains only one such tripeptide, Ile[72]-Glu[73]-Val[74], the stretch must correspond to Lys[70]–Val[74]. A unique dipeptide, X-F (Figure 9A), was assigned to Glu[75]-Phe[76]. This led to the sequence-specific assignment of Phe[76]; assignments of Lys[70] and Lys[71] were confirmed by $^1H\{^{13}C\}$ experiments (Wang et al., 1990).

A three-residue segment was located from $d_{\alpha N}$ connectivities (Figure 9A). It was assigned to His[8]-Lys[9]-Glu[10] on the basis of the unique -H-K- dipeptide (Figure 5). The assignments of histidine and lysine spin systems were confirmed by $^1H\{^{13}C\}$ experiments (Wang et al., 1990).

Several NOE's were observed between the protons of these two segments including one between the amide protons of Glu[10] and Val[74] (Figure 9B) and between the $^1H^{\alpha}$ of Lys[9] and the $^1H^{\alpha}$ Glu[75] (Figure 2B) Proline does not give rise to a cross peak in the fingerprint region; however, the $^1H^{\alpha}$ proton of proline yields a sequential $d_{\alpha N}$ NOE with the $^1H^N$ of the following residue. One strong NOE cross peak at 8.10,4.94 ppm (Figure 10A) connects the $^1H^N$ of Ala[12] (assigned later) to the $^1H^{\alpha}$ of Pro[11]. By following the $^1H^{\alpha}$ chemical shift of Pro[11], a $d_{\alpha\alpha}$ NOE was found between Pro[11] and Glu[73] (Figure 2D). A $^1H\{^{13}C\}$SBC-NOE experiment confirmed this identification (Wang et al., 1990). A weak d_{NN} NOE was observed between Ala[12] and Ile[72] (Figure 9B). Furthermore, as indicated in Figures 2D and 9B, the $^1H^N$ and $^1H^{\alpha}$ protons of the segment Ile[72]–Glu[75] show NOE's to the segment Tyr[91]–Ala[94]: d_{NN} connectivities between Glu[73] and Tyr[93] and between Glu[75] and Tyr[91]; $d_{\alpha N}$ connectivities between $^1H^{\alpha}$ of Ala[94] and $^1H^N$ of Glu[73]; $d_{\alpha\alpha}$ connectivities between Ile[72] and Ala[94] and between Val[74] and Ile[92]. This set of identified interstrand NOE's provides evidence that segment Ile[72]–Glu[75] is in the middle of three antiparallel strands, Lys[9]–Ala[12], Ile[72]–Glu[75], and Tyr[91]–Ala[94], and that, together with segment Ala[94]–Val[99], they form an antiparallel β-pleated sheet and reverse turn. The relative orientation of the strands within this β-sheet is presented schematically in Figure 12A.

(2) Antiparallel β-Sheet with Two Turns Involving the Segment from Ala[12] to Arg[35]. A sequence of ten residues was identified from a $d_{\alpha N}$ sequential walk as indicated in Figure 10. The sequence involves the tripeptide segment L-X-Y, which assigns it to the unique tripeptide Leu[25]-Met[26]-Tyr[27]

Table I: Resonance Assignments of Staphylococcal Nuclease H124L in Ternary Complex at 45 °C[a]

	$^1H^N$	$^1H^\alpha$	$^1H^\beta$	$^1H^\gamma$	$^1H^\delta$	$^1H^\epsilon$	$^1H^\zeta$	$^1H^\eta$
His 8	8.83	5.04	3.26; 3.33		7.34	8.66		
Lys 9	8.51	4.82	1.53					
Glu 10	9.29	5.06	2.16					
Pro 11		(4.94)			3.57; 3.92*			
Ala 12	8.09	5.01	1.34					
Thr 13	8.09	4.73	4.12	1.28				
Leu 14	9.08	4.13	1.93					
Ile 15	8.31	4.25	1.33	γ_1 1.35*	0.83*			
				γ_2 0.9*				
Lys 16	8.02	4.46	1.84					
Ala 17	9.37	4.45	1.37					
Ile 18	7.93	4.06	1.58	γ, 1.11; 1.44*	0.78*			
				γ_2 0.87*				
Asp 19	8.51	4.67						
Gly 20	(8.85)							
Asp 21	7.69	4.89						
Thr 22	7.70	5.64	3.97	1.16				
Val 23	9.15	4.65	1.93	0.78; 0.84				
Lys 24	9.44	5.44	2.02					
Leu 25	9.33	5.21	1.78					
Met 26	9.51	4.88	2.28; 1.75*	2.50*		1.97*		
Tyr 27	9.03	5.06*	3.01; 3.19		7.34*	6.92*		
Lys 28	9.25	3.60	1.38					
Gly 29	8.37	3.51; 4.14						
Gln 30	7.82	5.04	2.08					
Pro 31		(4.84)			3.20; 3.80*			
Met 32	9.50	4.65	1.98; 2.10	2.44*		1.90*		
Thr 33	8.86	4.49	3.98	0.95				
Phe 34	9.69	4.94*	2.37*; 2.89		6.91*	6.91*	6.64*	
Arg 35	9.84	4.99	1.92*					
Leu 36								
Leu 37		(3.92)						
Leu 38	9.32	4.31	1.91					
Val 39	6.94	5.74	1.87	0.73; 1.02				
Asp 40	8.88	5.22	2.48					
Thr 41		5.14*	4.23*	1.18*				
Pro 42					3.54; 3.71*			
Glu 43								
Thr 44	8.30	4.38	4.29	1.14				
Lys 45	8.13	4.24						
His 46	8.34	4.89	3.12; 3.17		7.30	8.29		
Pro 47								
Lys 48								
Lys 49								
Gly 50	8.23	3.84; 4.14*						
Val 51	8.02	4.10	2.08	0.95; 1.0				
Glu 52	8.24	4.29	1.73					
Lys 53								
Tyr 54		4.39*	3.18*		6.82*	6.73*		
Gly 55		3.80; 3.90*						
Pro 56					3.56; 3.63*			
Glu 57								
Ala 58	8.82	4.17	1.72					
Ser 59	8.30*	3.98	3.74					
Ala 60	8.25	4.05	1.51					
Phe 61	8.15	4.05*	3.14; 3.33		7.13*	7.22*	7.21*	
Thr 62	8.58	3.60	4.12	1.01				
Lys 63	8.04	3.58	1.77					
Lys 64	7.95	3.93	1.74					
Met 65	7.65	3.92	1.80; 2.16*	2.46*		1.94*		
Val 66	8.22	4.17	2.15	0.89; 1.15				
Glu 67	8.78	3.98	2.06					
Asn 68	7.32	4.69	2.78; 2.81					
Ala 69	6.68	4.52	1.32					
Lys 70	10.11	4.35	2.03					
Lys 71	8.85	4.66	1.74					
Ile 72	8.86	5.23	1.89	γ_1 1.15; 1.33	0.89*			
				γ_2 0.64*				
Glu 73	8.80	5.27	1.74					
Val 74	9.54	4.62	1.29	−0.14; 0.3				
Glu 75	8.82	5.15	2.91					
Phe 76	8.79	4.77*	2.92; 3.55*		7.69*	7.27*	6.79*	
Asp 77	9.26	5.32	3.83					
Lys 78	10.31	4.24	1.91					
Gly 79	8.64	3.33; 4.42						
Gln 80	8.68	4.14	2.00					
Arg 81	(8.55)	(4.16)	(2.05)					

Table I (Continued)

	$^1H^N$	$^1H^\alpha$	$^1H^\beta$	$^1H^\gamma$	$^1H^\delta$	$^1H^\epsilon$	$^1H^\zeta$	$^1H^\eta$
Thr 82	7.33	5.56	3.84	0.96				
Asp 83	8.75	4.64	2.36					
Lys 84	(8.67)							
Tyr 85	8.15	4.65*	2.88; 3.39*		7.02*	6.91*		
Gly 86	8.18*	3.61; 4.21						
Arg 87	8.67*	4.39	1.99					
Gly 88	8.80	2.68; 4.46						
Leu 89	8.32	5.21	1.70					
Ala 90	7.32	4.81	0.75					
Tyr 91	9.02	4.63*	3.40			6.58*		
Ile 92	7.79	4.97	1.46	γ_1 0.98; 1.17* γ_2 0.64*	0.34*			
Tyr 93	9.52	5.11*	2.84		6.63*	6.73*		
Ala 94	9.23	4.98	1.13					
Asp 95	9.65	4.43	2.74					
Gly 96	9.28	3.67; 4.25						
Lys 97	7.86	4.66	1.85					
Met 98	9.23	3.83	1.49*; 1.98	2.11*		1.44*		
Val 99	10.10	3.70	1.83	0.98; 1.05				
Asn 100	(9.58)	4.07	2.79; 2.93					
Glu 101	6.15	3.69	2.25					
Ala 102	7.84	4.08	1.69					
Leu 103	8.0	3.34	1.72					
Val 104	6.87	3.98	2.10	1.05				
Arg 105	9.04	4.03*	1.98*					
Gln 106	7.15	4.30	1.49					
Gly 107	8.01	4.01; 4.28						
Leu 108	7.76	4.33	1.99					
Ala 109	6.92	4.53	1.03					
Lys 110	7.59	5.11	1.83					
Val 111	9.13	4.71	1.99	0.85; 0.90				
Ala 112	7.92	4.17	0.80					
Tyr 113	7.78	3.44*	2.57*; 2.97		6.98*	6.74*		
Val 114	7.74	3.60	1.93	0.58; 0.71				
Tyr 115	8.97	5.03*	3.00; 3.11		7.15*	6.60*		
Lys 116	8.65	4.01	1.76					
Pro 117								
Asn 118	8.62	5.32	3.12					
Asn 119	8.15	5.04	2.18					
Thr 120	10.54	3.91	3.81	0.77				
His 121	6.93	5.47	2.35; 3.28*					
Glu 122	7.53	3.71	2.19					
Gln 123	8.87	4.00	2.14					
Leu 124	7.79	4.12	1.78*					
Leu 125	7.68	4.03	1.90					
Arg 126	8.90	4.00	1.98					
Lys 127	8.15	4.16	2.02					
Ser 128	7.75	4.33	4.10*					
Glu 129	8.47	3.90	2.20					
Ala 130	7.94	3.84	1.48					
Gln 131	7.45	4.00	2.20					
Ala 132	7.85	3.96	1.75					
Lys 133	8.17	3.41	1.25					
Lys 134	7.77	3.97	1.95					
Glu 135	7.59*	4.06	2.03					
Lys 136	7.81	3.54	2.06					
Leu 137	7.60*	4.19	1.52					
Asn 138	9.00	3.86	2.77					
Ile 139	8.34	3.32	1.05	γ_1 0.5; γ_2 0.12	0.06			
Trp 140	7.77	4.91	2.83; 3.71		7.0*	ϵ_3 7.66*	ζ_2 7.54 ζ_3 7.06*	7.12*
Ser 141	8.04	4.19	3.81; 3.87					
Glu 142	7.89	4.43	1.97; 2.19					
Asp 143	8.30	4.64	2.68; 2.78					

[a] Results from $^1H\{^{13}C,^{15}N\}$SBC-NOE experiments are indicated by asterisks (*); assignments from NOESY experiments alone (i.e., no independent identification of the spin system) are denoted by parentheses. Aliphatic proton chemical shifts were taken from COSY data. $^1H^N$ chemical shifts were obtained in H_2O; all others were obtained in ^2H_2O.

(Figure 5). Thus the sequence of ten residues corresponds to Asp[21]–Gln[30]. As shown in Figure 10A, residues Lys[24] and Lys[28] are connected by strong NOE's, and residues Lys[28] and Gln[30] are connected by weak NOE's (these overlap with intraresidue NOE cross peaks). A peptide of four residues was assigned to Met[32]–Arg[35] on the basis of the single remaining unassigned phenylalanine residue, Phe[34]. The specific assignment of Arg[35] was confirmed by $^1H\{^{13}C\}$SBC and ^1H-$\{^{13}C\}$SBC-NOE experiments with protein containing ^{13}C-labeled arginine (Wang et al., 1990). The $^1H^\alpha$–$^1H^\alpha$ connectivity region of the NOESY (^2H_2O) spectrum (Figure 2D) shows $d_{\alpha\alpha}$ NOE's between Thr[22] and Arg[35] and between Lys[24] and

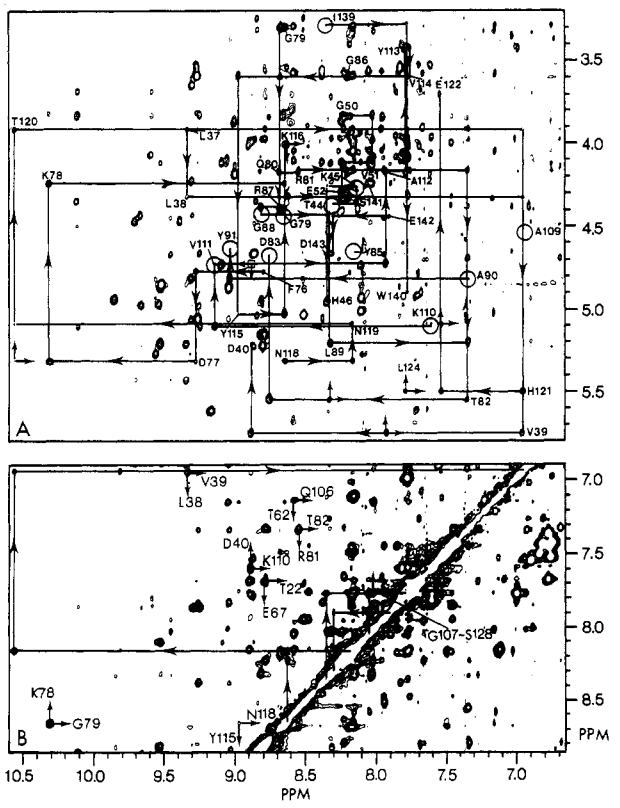

FIGURE 11: Evidence for the antiparallel β-sheet containing segments Leu[37]–Thr[41] and Ala[109]–Ala[112]. All the observed long-range NOE connectivities that provided information on the backbone conformation are indicated in the figure. (A) Sequential $d_{\alpha N}$ connectivities. The small square indicates the position of an NOE cross peak that appears at lower contour levels. (B) The d_{NN} connectivity region.

Thr[33]. Furthermore, d_{NN} NOE's were observed between amide protons of residues Val[23] and Phe[34] and between residues Leu[25] and Met[32] (Figure 10B). The $^1H^N$'s of Met[32] and Phe[34], in turn, show $d_{\alpha N}$ connectivities with the $^1H^\alpha$'s of Met[26] and Lys[24], respectively (Figure 10A). These results indicate that the segments Met[32]–Arg[35] and Thr[22]–Met[26] make up two adjacent antiparallel strands whose relative orientation is shown schematically in Figure 12B.

Starting from Met[26], a five-residue sequence of d_{NN} connectivities identifies the sequence Met[26]-Tyr[27]-Lys[28]-Gly[29]-Gln[30] (Figure 10B). The d_{NN} NOE's are strong between Lys[28] and Gly[29] and between Gly[29] and Gln[30], medium between Met[26] and Tyr[27], and weak between Tyr[27] and Lys[28]. The $d_{NN}(i,i+2)$ connectivities between Lys[28] and Gln[30] and between Tyr[27] and Gly[29] as well as the d_{NN} NOE between Tyr[27] and Gln[30] are indicated in Figure 10B. A $d_{\alpha N}(i,i+2)$ connectivity between Tyr[27] and Gly[29] also was observed (Figure 10A). These data show that Tyr[27]-Lys[28]-Gly[29]-Gln[30] forms a reverse turn.

Another $d_{\alpha N}$ walk starting from an alanine cross peak is indicated in Figure 10A. This segment is assigned to residues Ala[12]–Ala[17] on the basis of the unique six-residue sequence A-T-Z-I-Z-A. $^1H^\alpha$–$^1H^\alpha$ connectivities were found between Leu[14] and Leu[25] and between Ala[12] and Tyr[27] (Figure 2D). Since the $^1H^\alpha$ chemical shifts of Ala[12] and Tyr[27] are very close to one another, the $d_{\alpha\alpha}$ NOE cross peak is very close to the diagonal and thus difficult to observe. However, it shows up clearly in the $^1H\{^{13}C\}$SBC-NOE experiment (Wang et al., 1990). The d_{NN} NOE's between Thr[13] and Met[26] and between Ile[15] and Lys[24] (Figure 10B) and the $d_{\alpha N}$ NOE between the $^1H^\alpha$ of Leu[25] and the $^1H^N$ of Ile[15] (Figure 10A) together with all observed interstrand $d_{\alpha\alpha}$ NOE's reveal that residues Ala[12]–Ala[17] make up the third strand adjacent to the Thr[22]–Tyr[27] segment of the antiparallel β-sheet (Figure 12B).

A strong NOE was observed between the $^1H^N$ of Ile[15] and the $^1H^N$ of Lys[16] as well as a medium-range d_{NN} NOE between Lys[16] and Lys[24] (Figure 10B). These NOE's are not characteristic for β-sheet. It seems that the backbone of the strand Ala[12]–Ala[17] has some distortion at the position around Ile[15] and Lys[16].

As shown in Figure 10B, a strong d_{NN} cross peak starting from one of the isoleucine residues is assigned to the dipeptide Ile[18]-Asp[19]. A weak d_{NN} cross peak then extends the sequence of Gly[20]. The amide proton of Asp[19] also shows an NOE connectivity with Thr[22]. The corresponding $d_{\alpha N}$ connectivity between Ile[18] and Asp[19] is indicated in Figure 10A. Cross peaks from Gly[20] are missing in the fingerprint region of COSY and NOESY spectra. On the basis of the observed NOE's, it can be concluded that the segment Ile[18]–Asp[21] forms a reverse turn.

In summary, all the NOE connectivities within the long segment Ala[12]–Arg[35] indicate that these 24 residues form an antiparallel β-sheet of three strands and two turns as drawn schematically in Figure 12B.

(3) Antiparallel β-Pleated Sheet Involving the Segments Leu[37]–Thr[41] and Ala[109]–Ala[112]. One small segment, the unique tripeptide L-V-B defined by a $d_{\alpha N}$ sequential walk (Figure 11A), was assigned to Leu[38]-Val[39]-Asp[40]. A second stretch of seven residues, Z-V-A-Y-V-Y-Z (unique sequence), was identified from $d_{\alpha N}$ NOE connectivities (Figure 11A) and assigned to Lys[110]–Lys[116]. The assignments of Tyr[113], Tyr[115], Lys[110], and Lys[116] were confirmed by $^1H\{^{13}C\}$ experiments (Wang et al., 1990), while those of Val[111], Ala[112], and Val[114] were consistent with previous proton spin system identifications. Several NOE cross peaks were observed between these two segments. The $^1H^N$ of Lys[110] shows an NOE with the $^1H^N$ of Asp[40] (Figure 11B). The $^1H^\alpha$ of Val[39] shows an NOE with the $^1H^N$ of Ala[112], and the $^1H^\alpha$ of Val[111] shows an NOE with the $^1H^N$ of Asp[40]. In addition, strong $d_{\alpha\alpha}$ NOE's were observed between two pairs of residues: Val[39] and Val[111] and Thr[41] and Ala[109]. Although the Thr[41] cross peak is missing in ^1H spectra, the $^1H\{^{13}C\}$SBC-NOE spectrum shows the spin system of Thr[41] clearly and also provides evidence for an NOE between the $^1H^\alpha$'s of Thr[41] and Ala[109] (Wang et al., 1990). Analysis of the NOE connectivities of these two segments indicates that tripeptide Val[39]–The[41] forms one strand of an antiparallel β-sheet and that the opposite strand is made up by the segment Ala[109]–Ala[112] as shown schematically in Figure 12C.

As mentioned above, Leu[38] and Val[39] show a $d_{\alpha N}$ NOE connectivity. Figure 11A shows an NOE cross peak at 9.33,3.90 ppm that connects the $^1H^N$ of Leu[38] with the $^1H^\alpha$ of an unidentified residue. Figure 11B shows a d_{NN} connectivity between the amide protons of Leu[38] and Val[39]. If we make a tentative assignment of the missing cross peak to Leu[37], then we can make a schematic representation of segments Leu[37]–Thr[41] and Ala[109]–Ala[112] (Figure 12C).

Large Loop: Asn[77]–Ala[90]. A segment of five residues, B-Z-Y-G-Z, was found from d_{NN} connectivities in Figure 9B. On the basis of the unique tripeptide Y-G-R, this segment was assigned to Asp[83]–Arg[87]. The sequence-specific assignment of Gly[86] was consistent with prior spin system identification. The assigments of Tyr[85], Lys[84], and Arg[87] were confirmed by $^1H\{^{13}C\}$ experiments (Wang et al., 1990). A sequential $d_{\alpha N}$ walk (Figure 11A) extending from residue Phe[76] is assigned to the sequence Phe[76]–Gln[80]. A strong d_{NN} NOE was found between Lys[78] and Gly[79] (Figure 11B). Figure 11A shows a strong $d_{\alpha N}$ NOE between Asp[83] and Thr[82] and also an NOE

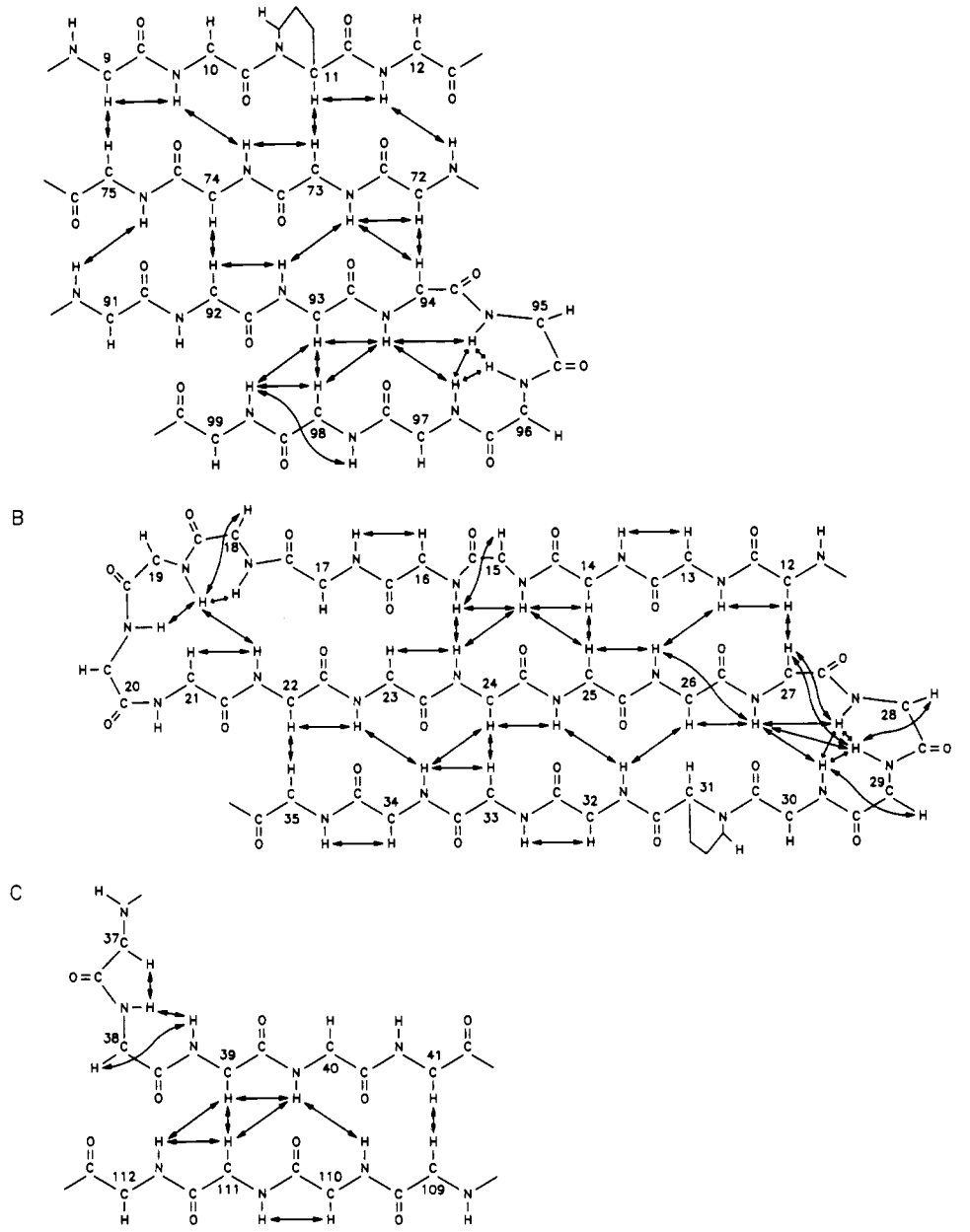

FIGURE 12: NMR analysis of antiparallel β-sheet and turn structures. NOESY connectivities used to establish the orientation of the strands are indicated by double arrows. (A) First β-sheet region identified in Figure 9. (B) Schematic representation of the second antiparallel β-sheet region. (C) Schematic drawing of the third antiparallel β-sheet.

cross peak at 7.35,4.16 ppm which connects the $^1H^N$ of Thr^{82} to the $^1H^\alpha$ of Arg^{81}. The corresponding d_{NN} connectivity between Arg^{81} and Thr^{82} was found in Figure 11B. Although the cross peak of Arg^{81} is missing from the fingerprint region, its position can be predicted from these NOE's to be 8.55,4.16 ppm. The sequence-specific assignments of Gly^{78} and Thr^{82} were consistent with their well-identified spin systems. The assignments of Lys^{78} and Arg^{81} were confirmed by $^1H\{^{13}C\}$-SBC-NOE experiments with protein samples labeled selectively with ^{13}C in lysine or arginine (Wang et al., 1990). The cross peak from residue Lys^{84} is missing in the fingerprint region. A third long $d_{\alpha N}$ sequential walk (Figure 11A) extended from Gly^{86} to Tyr^{91}. The sequence-specific assignments of Gly^{86} and Gly^{88} were consistent with previous spin system identifications, and the assignments of Arg^{87} and Leu^{89} were confirmed by heteronuclear NMR experiments (Wang et al., 1990). The sequences identified above can be linked together into a long sequence, Asn^{77}–Ala^{90}. The $^1H^\alpha$ of Thr^{82} builds up NOE's with the $^1H^\alpha$ of Gly^{88} (Figure 2D) and the $^1H^N$ of Leu^{89} (Figure 11A).

Analysis of all the observed NOE's within this long sequence reveals its backbone conformation. The sequence contains three turning points: Lys^{84}-Tyr^{85}, Arg^{81}-Thr^{82}, and Lys^{78}-Gly^{79}. The segments Lys^{84}-Arg^{87} and Lys^{78}-Gln^{80} form two reverse turns. Approximately midway between them, the sequence Arg^{81}–Asp^{83} makes up another turn. Thr^{82} is very close in space to Gly^{88} and Leu^{89}. Therefore, this long sequence forms a large "heart-shaped" loop.

Loop: *Tyr*^{115}–*His*^{121}. A four-residue segment, Asn^{118}-Asn^{119}-Thr^{120}-His^{121}, was identified as extending from the N-terminal of the α-helix Glu^{122}–Leu^{137} (Figure 11A). The corresponding d_{NN} connectivities of this segment were found in Figure 11B. Several additional NOE's involving this segment were observed including $d_{\alpha N}(i,i+3)$ connectivities between Asn^{119} and Glu^{122} and between His^{121} and Leu^{124} (Figure 11A), $d_{\alpha\beta}(i,i+3)$ connectivities between Asn^{119} and Glu^{122} and between Thr^{120} and Gln^{123} (Figure 2C), and a nonsequential $d_{\alpha N}(i,i+2)$ connectivity between Asn^{118} and Thr^{120} (Figure 11A). Since there is no sequential d_{NN} connectivity between His^{121} and Glu^{122} (Figure 5), the above NOE's indicate that

the segment Asn[118]–His[121] forms a segment of type III reverse turn. In addition, the $^1H^N$ of Asn[118] builds up NOE's with the $^1H^\alpha$ of Lys[116] (Figure 11A) and the $^1H^N$ of Tyr[115] (Figure 11B). This indicates the presence of a turn in the segment Tyr[115]–Asn[118]. Therefore, the segment Tyr[115]–His[121] forms a loop joining together the stretch of residues Lys[110]–Tyr[115] and the α-helix Glu[122]–Leu[137]. The NOE observed (Figure 11B) between amide protons of Gly[107] and Ser[128] indicates that the N-terminal of the segment Lys[110]–Tyr[115] is close to the middle of the α-helix.

Spatial Arrangement of β-Sheets and α-Helices. The peptide segment Ala[69]-Lys[70]-Lys[71] links the α-helix Ala[58]–Ala[69] with the N-terminal of the strand Ile[72]–Glu[75] of the antiparallel β-sheet. Figure 9B shows a strong NOE cross peak between the amide protons of Lys[70] and Lys[71]. Therefore, the linkage is not extended but is bent to form an antiparallel β-sheet with the segments Tyr[91]–Ala[94] and Lys[9]–Ala[12] (Figure 12A).

Long-range d_{NN} connectivities were observed between Thr[22] and Glu[67], Thr[62] and Gln[106] (Figure 11B), Lys[71] and Asp[95] (Figure 9B), Ala[69] and Val[99] (Figure 8B), Ala[90] and Lys[28], and Ala[90] and Tyr[27] (Figure 10B). Thr[62], Ala[69], Val[99], and Gln[106] are found in α-helices Ala[58]–Ala[69] and Met[98]–Ala[109]. The d_{NN} NOE's observed among these indicate that the C-terminal of α-helix Met[98]–Ala[109] is close in space to the N-terminal of α-helix Ala[58]–Ala[69] and that the C-terminal of α-helix Ala[58]–Ala[69] is close to the N-terminal of α-helix Met[98]–Ala[109]. Moreover, the first β-sheet (segments Lys[9]–Ala[12], Ile[72]–Glu[75], and Tyr[91]–Val[99]) and α-helix Met[98]–Ala[109] have a common amino acid residue, Val[99]. Segment Ala[90]–Val[99] contains a turn at residues Ala[94]–Lys[97] (Figure 12A), which is close in space to the bend at Lys[70]-Lys[71] on the basis of a d_{NN} connectivity between residues Lys[71] and Asp[95]. Therefore, α-helices Ala[58]–Ala[69] and Met[98]–Ala[109] are probably parallel and also close to one another in space.

The d_{NN} NOE between Thr[22] and Glu[67] indicates that the turn Ile[18]–Asp[21] of the second β-sheet is close to the C-terminal of α-helix Ala[58]–Ala[69]. Furthermore, the d_{NN} NOE's between Ala[90] and both Lys[28] and Tyr[27] show that turn Tyr[27]–Gln[30] of the second β-sheet is close to the junction of the first β-sheet with loop Asn[77]–Ala[90].

Short α-Helical Segment: Ile[139]–Asp[143]. Figure 11B shows a stretch of d_{NN} connectivities that starts from residue Ile[139]. This stretch involves five residues which are assigned readily to Ile[139]–Asp[143]. The assignments of Trp[140], Ser[141], and Asp[143] are consistent with previous spin system identifications. Since it contains only weak $d_{\alpha N}$ connectivities, between Ile[139] and Trp[140] and between Glu[142] and Asp[143] (Figure 11A), the segment Ile[139]–Asp[143] probably is a segment of α-helix.

Turn: Thr[44]–Glu[52]. Additional $d_{\alpha N}$ connectivities that involve three residues including His[46] are shown in Figure 11A. Corresponding weak d_{NN} connectivities are shown in Figure 9B. This segment is assigned to Thr[44]–His[46]. A three-residue segment of $d_{\alpha N}$ connectivities containing a valine (Figure 11A) is assigned to Gly[50]-Val[51]-Glu[52] since Val[51] is the only unidentified valine remaining. A d_{NN} connectivity was found between residues Glu[52] and Val[51] (Figure 9B). These NOE connectivities provide the backbone conformation of the segment Thr[44]–Glu[52]. Although, we were unable to identify several cross peaks in this region, it still can be concluded that this segment has two turning positions, at residues Thr[44]–His[46] and Gly[50]–Glu[52].

Conclusions

Staphylococcal nuclease–pdTp–Ca^{2+} ternary complexes are among the largest protein systems to be analyzed by NMR at this structural level. In our experience, the use of a 50% random fractionally deuterated protein sample (LeMaster & Richards, 1988) was critical to our success with $^1H\{^1H\}$ 2D spectroscopy. The resolution obtained in the fingerprint region was significantly better with 50% random fractionally deuterated nuclease than with nuclease at natural abundance. The resulting COSY (H_2O) and NOESY (H_2O) data provided sufficient information for the identification of secondary structural elements in the amino acid sequence. By combining these results with additional data from heteronuclear NMR experiments with ^{13}C- and ^{15}N-labeled protein samples (Wang et al., 1990), we were able to obtain sequence-specific assignments for 121 of the 149 amino acid residues of the ternary complex (Table I). About 45 $^1H^\alpha$–$^1H^N$ cross peaks remained 12 h after freshly prepared [na]H124L-TC was dissolved in ^2H_2O and incubated at 45 °C. Most of the slowly exchanging cross peaks were from the residues involved in secondary structural elements (Figure 5).

The 28 cross peaks that remain unassigned are from six amino acid residues in the C-terminal region, seven amino acids in the N-terminal region, and the segment Pro[42]–Glu[57]. We were unable to find NOE connectivities for these regions. Similar problems were encountered in the sequence-specific assignment of the nuclease wt ternary complex (Torchia et al., 1989). The chemical shifts of the assigned resonances from the nuclease H124L (present work) and nuclease wt (Torchia et al., 1989) ternary complexes are quite similar except for residues in the region of the mutation (residue 124). A detailed comparison of these data will be presented elsewhere. Experiments involving additional labeled protein analogues will be needed to complete the missing assignments and to provide stereospecific assignments.

The backbone conformation and the global fold discussed above, however, show clearly that the solution structure of H124L-TC as derived independently from NMR data (Figure 5) corresponds closely to the crystal structure of the ternary complex made from wild-type nuclease (Cotton et al., 1979). Figure 5 presents a summary of secondary structural elements in solution as determined by NMR analysis. The spectroscopic results reported here provide the groundwork for assignments for unligated nuclease H124L and for structural and dynamic studies of the numerous interesting mutants of staphylococcal nuclease that are available (Shortle et al., 1988; Alexandrescu et al., 1989; A. T. Alexandrescu, A. P. Hinck, and J. L. Markley, unpublished results).

Acknowledgments

We thank Dr. Dennis A. Torchia for sending copies of his manuscripts prior to publication.

References

Alexandrescu, A. T., Mills, D. A., Ulrich, E. L., Chinami, M., & Markley, J. L. (1988) *Biochemistry 27*, 2158–2165.

Alexandrescu, A. T., Ulrich, E. L., & Markley, J. L. (1989) *Biochemistry 28*, 204–211.

Anfinsen, C. B. (1973) *Science 181*, 223–230.

Anil Kumar, Ernst, R. R., & Wüthrich, K. (1980) *Biochem. Biophys. Res. Commun. 95*, 1–6.

Bax, A., & Davis, D. G. (1985) *J. Magn. Reson. 65*, 355–360.

Bax, A., & Drobny, G. (1985) *J. Magn. Reson. 61*, 306–320.

Billeter, M., Braun, W., & Wüthrich, K. (1982) *J. Mol. Biol. 155*, 321–346.

Bodenhausen, G., Kogler, H., & Ernst, R. R. (1984) *J. Magn. Reson. 58*, 370–388.

Bundi, A., & Wüthrich, K. (1979) *Biopolymers 18*, 285–297.

Calderon, R. O., Stolowich, N. J., Gerlt, J. A., & Sturtevant, J. M. (1985) *Biochemistry 24*, 6044–6049.

Chazin, W. J., & Wüthrich, K. (1987) *J. Magn. Reson. 72*, 358–363.
Cotton, F. A., Hazen, E. E., Jr., & Legg, M. J. (1979) *Proc. Natl. Acad. Sci. U.S.A. 76*, 2551–2555.
Cusumano, C. L., Taniuchi, H., & Anfinsen, C. B. (1968) *J. Biol. Chem. 243*, 4769–4774.
Englander, S. W., & Wand, A. J. (1987) *Biochemistry 26*, 5953–5958.
Evans, P. A., Dobson, C. M., Kautz, G. H., & Fox, R. O. (1987) *Nature 329*, 266–268.
Evans, P. A., Kautz, R. A., Fox, R. O., & Dobson, C. M. (1989) *Biochemistry 28*, 362–370.
Fox, R. O., Evans, P. A., & Dobson, C. M. (1986) *Nature 320*, 192–194.
Grissom, W. B., & Markley, J. L. (1989) *Biochemistry 28*, 2116–2124.
Hibler, D. W., Stolowich, N. J., Reynolds, M. A., Gerlt, J. A., Wilde, J. A., & Bolton, P. H. (1987) *Biochemistry 26*, 6278–6286.
Hynes, T. R., Kautz, R. A., Goodman, M. A., Gill, J. F., & Fox, R. O. (1989) *Nature 339*, 73–76.
Jardetzky, O., Markley, J. L., Williams, M. N., Thielmann, H., & Arata, Y. (1972) *Cold Spring Harbor Symp. Quant. Biol. 36*, 257–261.
LeMaster, D. M., & Richards, F. M. (1988) *Biochemistry 27*, 142–150.
Loll, P. J., & Lattman, E. E. (1989) *Proteins: Struct., Funct., Genet. 5*, 183–201.
Loll, P. J., Meeker, A. K., Shortle, D., Pease, M., & Lattman, E. E. (1988) *J. Biol. Chem. 263*, 18190–18192.
Macura, S., Wüthrich, K., & Ernst, R. R. (1982) *J. Magn. Reson. 46*, 269–282.
Marion, D., & Wüthrich, K. (1983) *Biochem. Biophys. Res. Commun. 113*, 967–974.
Markley, J. L., Putter, I., & Jardetzky, O. (1968) *Science 161*, 1249–1251.
Markley, J. L., Williams, M. N., & Jardetzky, O. (1970) *Proc. Natl. Acad. Sci. U.S.A 65*, 645–651.
McCain, D. C., Ulrich, E. L., & Markley, J. L. (1988) *J. Magn. Reson. 80*, 296–305.
Neuhaus, D. D., Wagner, G., Vasak, M., Kagi, J. H. R., & Wüthrich, K. (1985) *Eur. J. Biochem. 151*, 257–273.
Rance, M., Sørensen, O. W., Bodenhausen, G., Wagner, G., Ernst, R. R., & Wüthrich, K. (1983) *Biochem. Biophys. Res. Commun. 117*, 479–485.
Richardson, J. S. (1981) *Adv. Protein Chem. 34*, 167–339.
Rosenberg, A. H., Lade, B. N., Chui, D. S., Liu, S. W., Dunn, J. J., & Studier, F. W. (1987) *Gene 56*, 125–135.
Serpersu, E. H., Shortle, D., & Mildvan, A. S. (1987) *Biochemistry 26*, 1289–1300.
Shortle, D. (1983) *Gene 22*, 181–189.
Shortle, D. (1986) *J. Cell. Biochem. 30*, 281–289.
Shortle, D., & Lin, B. (1985) *Genetics 110*, 539–555.
Shortle, D., & Meeker, A. K. (1986) *Proteins 1*, 81–89.
Shortle, D., & Meeker, A. K. (1989) *Biochemistry 28*, 936–944.
Shortle, D., Meeker, A. K., & Friere, E. (1988) *Biochemistry 27*, 4761–4768.
Stanczyk, S. M., Bolton, P. H., Dell'Acqua, M., Pourmotabbed, T., & Gerlt, J. A. (1988) *J. Am. Chem. Soc. 110*, 7908–7910.
Stockman, B. J., Reily, M. D., Westler, W. M., Ulrich, E. L., & Markley, J. L. (1989) *Biochemistry 28*, 230–236.
Studier, F. W., & Moffatt, B. A. (1986) *J. Mol. Biol. 189*, 113–130.
Takahara, M., Hibler, D. W., Barr, P. J., Gerlt, J. A., & Inouye, M. (1985) *J. Biol. Chem. 260*, 2670–2674.
Torchia, D. A., Sparks, S. W., & Bax, A. (1988) *J. Am. Chem. Soc. 110*, 2320–2321.
Torchia, D. A., Sparks, S. W., & Bax, A. (1989) *Biochemistry 28*, 5509–5524.
Uhlmann, E., & Smith, J. A. (1987) *Nucleosides Nucleotides 6*, 331–334.
Wagner, G. (1983) *J. Magn. Reson. 55*, 151–156.
Wagner, G., Neuhaus, D., Wörgötter, E., Vasak, M., Kagi, J. H. R., & Wüthrich, K. (1986) *J. Mol. Biol. 187*, 131–135.
Wang, J., Hinck, A. P., Loh, S. N., & Markley, J. L. (1990) *Biochemistry* (following paper in this issue).
Wilde, J. A., Bolton, P. H., Dell'Acqua, M., Hibler, D. W., Pourmotabbed, T., & Gerlt, J. A. (1988) *Biochemistry 27*, 4127–4132.
Wüthrich, K. (1986) *NMR of Proteins and Nucleic Acids*, Wiley, New York.